

## Quantum dynamics in potentials with fast spatial oscillations

Viktor Novičenko,<sup>\*</sup> Julius Ruseckas,<sup>†</sup> and Egidijus Anisimovas<sup>‡</sup>

*Institute of Theoretical Physics and Astronomy, Vilnius University, Saulėtekio Ave. 3, LT-10257 Vilnius, Lithuania*



(Received 18 December 2018; published 5 April 2019)

We consider quantum dynamics of systems with fast spatial modulation of the Hamiltonian. Employing the formalism of supersymmetric quantum mechanics and decoupling fast and slow spatial oscillations we demonstrate that the effective dynamics is governed by a Schrödinger-like equation of motion and obtain the expression of the resulting effective Hamiltonian. In particular, we show that there exists an attractive effective potential even in the case when the oscillating potential averages to zero.

DOI: [10.1103/PhysRevA.99.043608](https://doi.org/10.1103/PhysRevA.99.043608)

### I. INTRODUCTION

The idea to simplify the analysis of a physical problem by taking into account the presence of substantially different characteristic scales (spatial, temporal, or other) is a ubiquitous and powerful one. Far-reaching examples include the Born–Oppenheimer approach [1,2], based on decoupling of fast and slow vibrational modes, and Floquet engineering [3], which fruitfully exploits the idea to realize effective Hamiltonians with desired properties by applying a time-periodic driving to a controllable physical system [4]. In the limit when the periodic driving sets the dominant frequency scale (in comparison with the internal dynamics of the system) the resulting (stroboscopic) dynamics is described by the time-averaged driven Hamiltonian. Already this rather simple result has led to numerous insights and ground-breaking experimental schemes [5–10]. When the driving sets the largest but not overwhelming frequency scale, the resulting dynamics may be captured by a systematic inverse-frequency expansion [11–13], which also offers opportunities for quantum engineering of physically interesting model Hamiltonians [14,15].

In the present contribution, we look at the complementary facet of *spatial*, rather than temporal, modulation of the Hamiltonian. We show that in the limit of rapid oscillations of the potential, the effective dynamics is governed by a Schrödinger-like equation of motion. The main contribution to the effective potential featured in this equation is proportional to the square of the envelope function that modulates the rapid oscillations of the true potential. Moreover, this contribution comes with a negative sign, i.e., there exists an attractive effective potential even when the oscillating potential averages to zero. The effective Schrödinger equation is solved by a smoothed wave function which accurately approximates the overall shape of the true wave function but excludes its rapid small-scale oscillations. The obtained description is relevant to describe quantum dynamics in potentials formed by interfering laser beams. Here, the resulting intensity distributions,

which define the potentials felt by ultracold atoms, typically combine rapid variations on the scale of the wavelength with slow modulation due to the shape of the beams [16].

Interestingly, in the derivation of the effective Schrödinger equation we benefited from an approach based on supersymmetric quantum mechanics (SUSY QM). SUSY QM is a generalization of the factorization method commonly used for the harmonic oscillator. It was first introduced as a model to study nonperturbative symmetry breaking in supersymmetric field theories [17]. Later it was realized that SUSY QM is an interesting field in its own right, and the ideas of supersymmetry have been profitably applied to many quantum-mechanical problems; see Refs. [18–20] for books and reviews.

Our paper is organized as follows: In Sec. II we derive the expression for the effective potential in a system with fast spatial potential modulation. To verify the validity of the effective Hamiltonian, in Sec. III we compare numerically calculated eigenfunctions of the original Hamiltonian with the eigenfunctions obtained by using the effective Hamiltonian. In Sec. IV we discuss applications to potentials for ultracold atoms formed by interfering laser beams. Finally, in Sec. V we summarize our findings.

### II. DYNAMICS IN A SPATIALLY MODULATED POTENTIAL

We study the motion of a one-dimensional quantum particle of mass  $m$  in a static spatially modulated potential  $V(x)$  whose shape can be represented as a combination of a slowly varying envelope function  $\Phi(x)$  with vanishing limiting values,

$$\lim_{x \rightarrow \pm\infty} \Phi(x) = 0, \quad (1)$$

and a periodic function  $v(kx) = v(kx + 2\pi)$ . The period of the rapid oscillations of the potential is given by  $2\pi/k$  and by assumption must be much smaller than the characteristic length scale of the envelope function  $\Phi(x)$ . The dynamics of the particle is described by the Schrödinger equation

$$i\hbar \frac{\partial}{\partial t} \psi = \hat{H} \psi, \quad (2)$$

<sup>\*</sup>viktor.novicenko@tfai.vu.lt; <http://www.itpa.lt/~novicenko/>

<sup>†</sup>julius.ruseckas@tfai.vu.lt; <http://web.vu.lt/tfai/j.ruseckas/>

<sup>‡</sup>egidijus.anisimovas@ff.vu.lt

with the Hamiltonian

$$\hat{H} = -\frac{\hbar^2}{2m} \frac{\partial^2}{\partial x^2} + V(x). \quad (3)$$

Our goal is to derive an effective Hamiltonian that approximates the ensuing dynamics for large but finite  $k$  and becomes exact in the limit  $k \rightarrow \infty$ . The potential-energy term is taken of the form

$$V(x) = kv(kx)\Phi(x) + \rho(x). \quad (4)$$

Here,  $v(s)$  is a periodic function that averages to zero over a period

$$\langle v \rangle = \frac{1}{2\pi} \int_0^{2\pi} v(s) ds = 0, \quad (5)$$

and in Eq. (4) is additionally scaled by a factor  $k$ ; that is, the increasing frequency of spatial oscillations is complemented by increasing amplitude. As further explained below, if this was not done, in the limit  $k \rightarrow \infty$ , the oscillatory potential  $v(kx)\Phi(x)$  would average out. The presence of a finite potential background is taken into account by a separate term  $\rho(x)$ , which is also required to vanish for  $|x| \rightarrow \infty$ ; cf. Eq. (1). To be able to work with dimensionless quantities, we identify a characteristic length scale  $\ell$  and measure coordinates in units of  $\ell$ , wave numbers in  $\ell^{-1}$ , energies in units of  $\hbar^2/(2m\ell^2)$ , and time in  $2m\ell^2/\hbar$ . The dimensionless Schrödinger equation reads

$$i \frac{\partial}{\partial t} \psi = \left\{ -\frac{\partial^2}{\partial x^2} + kv(kx)\Phi(x) + \rho(x) \right\} \psi(x, t). \quad (6)$$

We note that a related problem, as a specific case, was studied in Ref. [21], where ponderomotive dynamics was derived as an expansion with respect to the inverse wave number  $k^{-1}$ . However, here we are interested in the regime of large oscillation amplitude [in comparison to the particle-recoil energy  $\hbar^2/(2m\ell^2)$ ]. This regime cannot be directly covered by the formalism developed in Ref. [21].

#### A. Derivation of the effective Hamiltonian by using SUSY QM formalism

We derive the effective Hamiltonian by using an approach based on the formalism of SUSY QM (see, for example, Ref. [18]) and the subsequent application of the ‘‘averaging’’ theorem [22,23], which is a versatile tool that allows us to eliminate rapidly oscillating terms in broad classes of first-order differential-equation sets. (An alternative derivation is included as an Appendix.) To proceed, we write the Hamiltonian in a factorized form,

$$\hat{H} = \hat{A}^\dagger \hat{A}, \quad (7)$$

where

$$\hat{A} = \frac{\partial}{\partial x} + W(x), \quad (8)$$

and we introduced the superpotential  $W(x)$  as a solution of the differential equation

$$\frac{d}{dx} W(x) = W^2(x) - kv(kx)\Phi(x) - \rho(x), \quad (9)$$

which is known as the Riccati equation. Then we can replace the Schrödinger Eq. (6) by a pair of first-order differential equations

$$\frac{\partial}{\partial x} \psi(x, t) = \varphi(x, t) - W(x)\psi(x, t), \quad (10a)$$

$$\frac{\partial}{\partial x} \varphi(x, t) = -i \frac{\partial \psi(x, t)}{\partial t} + W(x)\varphi(x, t), \quad (10b)$$

which govern the wave function  $\psi(x, t)$  and an auxiliary function  $\varphi(x, t) = \hat{A}\psi(x, t)$ .

To be fully compliant with the requirements of the averaging theorem one should replace the partial derivatives  $\partial/\partial x$  with the full derivatives  $d/dx$ . Formally, this can be done by discretizing the time interval into small steps of duration  $\Delta t$  and introducing the notation  $\psi_{(m)}(x) \equiv \psi(x, m\Delta t)$  and  $\varphi_{(m)}(x) \equiv \varphi(x, m\Delta t)$ . Then the term  $\partial\psi(x, t)/\partial t$  can be approximated by a finite difference  $\partial\psi(x, m\Delta t)/\partial t \approx [\psi_{(m+1)} - \psi_{(m)}]/\Delta t$ . As a consequence, Eqs. (10) turns into set of differential equations for the functions  $\psi_{(m)}(x)$  and  $\varphi_{(m)}(x)$  formulated in terms of full derivatives with respect to the single variable  $x$ . However, to keep the notation simple we retain the partial derivatives having in mind that their presence poses no practical problems.

The three functions  $W$ ,  $\psi$ , and  $\varphi$  comprise the new dynamical variables and are governed by the set of first-order nonlinear differential Eqs. (9) and (10). Before proceeding to the averaging procedure, let us review the scaling of the potential energy, which we choose to write as  $kv(kx)\Phi(x)$ . At this stage we are in a position to see that—in the absence of the additional scaling by the factor  $k$ —the term  $v(kx)\Phi(x)$  would be eliminated from Eq. (9) by the averaging procedure as a rapidly oscillating term. In the presence of the scaling factor  $k$ , the potential energy  $kv(kx)\Phi(x)$  becomes formally divergent in the  $k \rightarrow \infty$  limit and must be cast into a manageable form. To achieve this aim, we replace  $W$  with a new variable

$$W' = W + g(kx)\Phi(x), \quad (11)$$

where the function  $g(s)$  is the zero-average antiderivative of the function  $v(s)$ , i.e.,

$$g(s) = \int_0^s v(s') ds' - \frac{1}{2\pi} \int_0^{2\pi} \int_0^{s''} v(s') ds' ds''. \quad (12)$$

The purpose of the transformation from  $W$  to  $W'$  can be elucidated by differentiating both sides of Eq. (11) with the result

$$\frac{d}{dx} W + kv(kx)\Phi(x) = \frac{d}{dx} W' - g(kx) \frac{d}{dx} \Phi(x), \quad (13)$$

demonstrating the absorption of the term proportional to  $k$ . Thus, the new variables  $W'$ ,  $\psi$ , and  $\varphi$  obey the differential equations

$$\frac{dW'}{dx} = [W' - g(kx)\Phi(x)]^2 - \rho(x) + g(kx) \frac{d\Phi}{dx}, \quad (14a)$$

$$\frac{\partial \psi}{\partial x} = \varphi - [W' - g(kx)\Phi(x)]\psi, \quad (14b)$$

$$\frac{\partial \varphi}{\partial x} = -i \frac{\partial \psi}{\partial t} + [W' - g(kx)\Phi(x)]\varphi. \quad (14c)$$

Here we consider continuous envelope functions  $\Phi(x)$  so that the spatial derivative of the envelope represented by the term  $d\Phi/dx$  in Eq. (14a) remains finite. The more general case of piecewise continuous envelope functions is treated in the following Sec. II B.

Now one can apply the averaging theorem [22,23]. In general, the averaging theorem can be formulated as follows: Let us consider the vector  $\mathbf{Z}(x)$  obeying the differential equation of the form

$$\frac{d\mathbf{Z}}{dx} = \mathbf{F}(\mathbf{Z}, kx, x, k), \quad (15)$$

where the vector field  $\mathbf{F}$  is  $2\pi$  periodic with respect to the second argument, slowly depends (in comparison to the characteristic period  $2\pi/k$ ) on the third argument, and additionally depends on the parameter  $k$  represented by the fourth argument. One can introduce the averaged vector field as

$$\bar{\mathbf{F}}(\mathbf{Z}, x) = \frac{1}{2\pi} \int_0^{2\pi} [\lim_{k \rightarrow \infty} \mathbf{F}(\mathbf{Z}, \vartheta, x, k)] d\vartheta. \quad (16)$$

According to the averaging theorem, the solution  $\bar{\mathbf{Z}}$  of the differential equation

$$\frac{d\bar{\mathbf{Z}}}{dx} = \bar{\mathbf{F}}(\bar{\mathbf{Z}}, x), \quad (17)$$

with the identical initial conditions  $\mathbf{Z}(x_0) = \bar{\mathbf{Z}}(x_0)$  approximates the original solution  $\mathbf{Z}(x) = \bar{\mathbf{Z}}(x) + O(k^{-1})$ . Thus from Eqs. (14) one finds

$$\frac{d\bar{W}'}{dx} = \bar{W}'^2 + \langle g^2 \rangle \Phi^2(x) - \rho(x), \quad (18a)$$

$$\frac{\partial \bar{\psi}}{\partial x} = \bar{\varphi} - \bar{W}' \bar{\psi}, \quad (18b)$$

$$\frac{\partial \bar{\varphi}}{\partial x} = -i \frac{\partial \bar{\psi}}{\partial t} + \bar{W}' \bar{\varphi}, \quad (18c)$$

where the averaged functions approximate the original functions as

$$\{\bar{W}', \bar{\psi}, \bar{\varphi}\} = \{W', \psi, \varphi\} + O(k^{-1}). \quad (19)$$

We note here that the use of two distinct notations for ‘‘averaging’’ is justified by their distinct meanings: the brackets  $\langle v \rangle$  refer to the mean value of a periodic function  $v$  taken over its period, whereas the overline  $\bar{\psi}$  refers to a smoothed approximation of an oscillatory function; cf. Fig. 1.

Finally, transforming Eqs. (18) back to a single second-order equation for the smoothed function  $\bar{\psi}$ , we obtain

$$i \frac{\partial \bar{\psi}}{\partial t} = -\frac{\partial^2}{\partial x^2} \bar{\psi} + V_{\text{eff}}(x) \bar{\psi}, \quad (20)$$

with

$$V_{\text{eff}}(x) = -\langle g^2 \rangle \Phi^2(x) + \rho(x). \quad (21)$$

This result shows that the dynamics is governed by an effective equation of motion which retains the form of the usual Schrödinger equation with the effective Hamiltonian

$$\hat{H}_{\text{eff}} = -\frac{\partial^2}{\partial x^2} + V_{\text{eff}}(x), \quad (22)$$

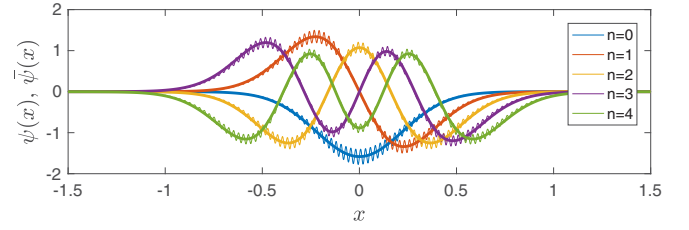


FIG. 1. The five lowest-energy states calculated numerically by using the original Hamiltonian (6) (thin oscillating curves) and found analytically for the effective Hamiltonian (25) (thick curves). The ground-state wave function is nodeless, and the excited states can be identified by the number of nodes. The parameters are set to  $k = 250$  and  $a = 2\sqrt{210}$  such that  $\lambda = 20$  is an integer number.

where the effective potential (21) includes an attractive contribution proportional to the *square* of the envelope function. In hindsight, this is intuitively clear: if there is no background, i.e.,  $\rho(x) = 0$ , the sign of the envelope function has no effect and only even powers of  $\Phi(x)$  can contribute. Finally, let us stress that even though the wave function  $\bar{\psi}$  approximates the original wave function  $\psi$  with the same accuracy as Eq. (19), i.e.,  $\bar{\psi} = \psi + O(k^{-1})$ , an analogous statement *does not hold* for either the kinetic energy or the potential energy calculated by using  $\bar{\psi}$ . Only the total energy is well approximated by the quantum-mechanical expectation value of the effective Hamiltonian with the smoothed wave function  $\bar{\psi}$ .

## B. Effective potential for piecewise continuous envelope

Discontinuous envelope functions do not satisfy the requirement that the characteristic length scale of the envelope function should be much larger than the period of the rapid oscillations. Thus the effective potential (21) is valid only for continuous envelope functions  $\Phi(x)$ . In this section we generalize our approach to include the case when the envelope is a piecewise continuous function. In this situation, the averaging is still applicable; however, at the points of discontinuity the smoothed functions  $\bar{\psi}$  must obey appropriate boundary conditions.

For each coordinate  $x$  which is not a point of discontinuity, all of the steps (9)–(18) can be repeated in exactly the same way as before. However, the points of discontinuity should be considered separately. At every point of discontinuity  $x_0$  the superpotential  $W(x)$  must remain continuous for any value of  $k$  [cf. Eq. (9)]. Using Eq. (11) for the transformed superpotential  $W'$  we obtain

$$\lim_{\varepsilon \rightarrow +0} [W'(x_0 + \varepsilon) - W'(x_0 - \varepsilon)] = g(\varphi_0) \Delta \Phi(x_0), \quad (23)$$

where  $\varphi_0 = kx_0$  is the phase of the oscillating function  $g(kx)$  at the point of discontinuity,  $x_0$ , and  $\Delta \Phi(x_0) = \lim_{\varepsilon \rightarrow +0} [\Phi(x_0 + \varepsilon) - \Phi(x_0 - \varepsilon)]$ . This result indicates that, at each point of discontinuity, the transformed superpotential exhibits a step given by the product of the step of the envelope function and the local value of the periodic antiderivative  $g(kx)$ . As a special case, the transformed superpotential may remain continuous if  $g(kx_0) = 0$ .

We must now require that  $k$  grows to infinity in discrete steps, i.e., by assuming a sequence of monotonically growing

values for which the phase  $\varphi_0$  remains the same (modulo  $2\pi$ ). Then the condition (23) will also hold for the averaged superpotential  $\bar{W}^i(x)$  and can be satisfied by including terms proportional to the Dirac  $\delta$  function  $\Delta\Phi(x_0)g(\varphi_0)\delta(x-x_0)$  to Eq. (18a). If there are several points of discontinuity  $\{x_n\}$  and it is possible to find values of  $k$  that keep the phases  $\varphi_n$  constant, the effective potential (21) becomes

$$V_{\text{eff}}(x) = -\langle g^2 \rangle \Phi^2(x) + \rho(x) - \sum_n \Delta\Phi(x_n)g(\varphi_n)\delta(x-x_n). \quad (24)$$

We see that step discontinuities in the envelope function translate into  $\delta$ -function singularities in the effective potential. As a special case, these singularities may be absent if  $g(\varphi_n) = 0$ .

### III. NUMERICAL EXAMPLES

To verify the validity of the effective description we perform a numerical calculation of the eigenfunctions for the original Hamiltonian (6) and compare them with the eigenfunctions obtained using the effective Hamiltonian (20). We treat both cases of continuous and piecewise continuous envelope functions and use the effective potentials given, respectively, by Eqs. (21) and (24).

Starting with the simpler case of a smooth envelope, the rapid potential oscillations are taken to have a harmonic shape; thus,  $v(s) = \cos(s)$  and its antiderivative  $g(s) = \sin(s)$  with  $\langle g^2 \rangle = 1/2$ . For the sake of convenience, the envelope function is described by  $\Phi(x) = a \operatorname{sech}(x)$ . Then the potential well has a characteristic width of order unity, and the effective Schrödinger equation for the averaged wave function

$$\bar{E} \bar{\psi}(x) = \left[ -\frac{d^2}{dx^2} - \frac{a^2}{2} \operatorname{sech}^2(x) \right] \bar{\psi}(x) \quad (25)$$

is solvable analytically. The eigenvalue problem (25) is known as the Pöschl-Teller problem [24], and the spectrum of the bound states is given by

$$\bar{E}_n = -(\lambda - n)^2. \quad (26)$$

Here, the parameter  $\lambda = (\sqrt{1+2a^2} - 1)/2$  is a function of the depth  $a$  and its integer part  $[\lambda]$  (i.e., the largest integer smaller than or equal to  $\lambda$ ) is equal to the number of bound states plus one. The index  $n = 0, 1, \dots, [\lambda] - 1, [\lambda]$  labels the bound states.

The comparison of the first five eigenfunctions of the original and the effective Hamiltonians is represented in Fig. 1. For convenience we choose the value of  $a$  such that  $\lambda$  becomes an integer number. In that case the eigenfunctions  $\bar{\psi}(x) \sim P_{\lambda-n}^{\lambda-n}(\tanh(x))$ , where  $P_{\lambda}^{\beta}(y)$  are the associated Legendre polynomials which are related to the ordinary Legendre polynomials  $P_{\lambda}(y)$  as

$$P_{\lambda}^{\beta}(y) = (-1)^{\beta} (1-y^2)^{\beta/2} \frac{d^{\beta}}{dy^{\beta}} P_{\lambda}(y). \quad (27)$$

In Fig. 2, we plot dependence of the eigenenergies on the potential amplitude parameter  $a$ . As one can see in Figs. 1 and 2, the approximate expression obtained by using the effective Hamiltonian shows good coincidence with the results of numerical calculations.

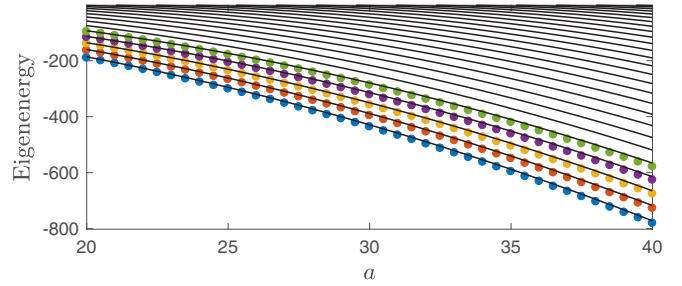


FIG. 2. The dependence of the lowest eigenenergies of the bound states on the depth of the potential well  $a$  for fixed  $k = 250$ . Solid curves are drawn from Eq. (26), while the circles are calculated numerically by using the original Hamiltonian (6).

To give an example of a piecewise continuous envelope, we consider the envelope function of the form of a square barrier:

$$\Phi(x) = \begin{cases} a & \text{for } |x| < 1 \\ 0 & \text{for } |x| > 1. \end{cases} \quad (28)$$

According to Eq. (24), the effective potential (21) reads

$$V_{\text{eff}}(x) = -\langle g^2 \rangle \Phi^2(x) + a[g(\varphi_1)\delta(x-1) - g(\varphi_{-1})\delta(x+1)], \quad (29)$$

with  $\varphi_{\pm 1} = \pm 1 \cdot k$ , and features two  $\delta$ -function terms at the points of discontinuity.

We perform numerical simulations with the high-frequency profile function  $v(s) = \cos(s)$ , which gives  $g(s) = \sin(s)$ . We choose an appropriate value of  $k$  to ensure  $\varphi_{\pm 1} = 0$ , and the effective potential (29) has the shape of an ordinary symmetric quantum well of finite depth  $a^2/2$ . The comparison of the first five eigenfunctions of the original and the effective Hamiltonian is presented in Fig. 3. We note an excellent agreement of the two sets of results, which demonstrates the applicability of the approach.

To demonstrate the asymmetric and singular case, we use  $v(s) = \sin(s)$  whose antiderivative is  $g(s) = -\cos(s)$ . Again, we set  $\varphi_{\pm 1} = 0$ , but now the effective potential (29) has the shape of a square quantum well with two extra  $\delta$ -function peaks situated at the edges: A repulsive (attractive)  $\delta$ -function peak of strength  $a$  is centered at  $x = -1$  ( $x = 1$ ). Figure 4

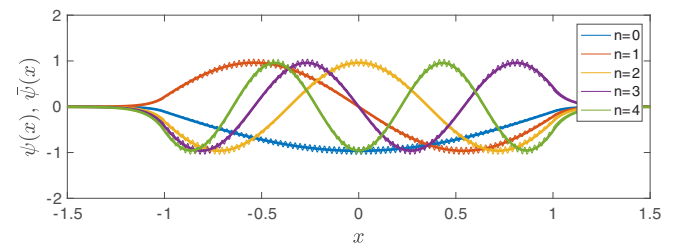


FIG. 3. The case of a piecewise continuous envelope (28). The five lowest-energy states are calculated numerically by using the original Hamiltonian (6) (thin oscillating curves) and found semi-analytically for the effective potential (29) (thick curves). The ground-state wave function is nodeless, and the excited states can be identified by the number of nodes. The parameters are set to  $a = 20$  and  $k \approx 250$  is chosen in such a way that  $g(\varphi_{-1,1})$  vanishes.

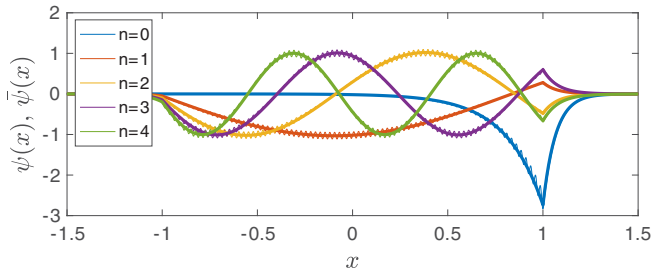


FIG. 4. The case of piecewise continuous envelope (28). The five lowest-energy states calculated numerically by using the original Hamiltonian (6) (thin oscillating curves) and found semi-analytically for the effective potential (29) (thick curves). The ground-state wave function is nodeless and decays exponentially on either side of the attractive  $\delta$ -function potential situated at  $x = 1$ . The excited states can be identified by the number of nodes. The parameters are set to  $a = 20$ , and  $k \approx 250$  is chosen in such a way that  $g(\varphi_{-1,1}) = -1$ .

again shows an excellent agreement between the exact numerical calculation and the results obtained by using the effective potential. As expected from Eq. (29), the probability density is increased close to the right side of the potential well, i.e., at the position of the attractive  $\delta$ -function singularity.

#### IV. OVERLAPPING LASER BEAMS

The preceding analysis shows that the case of oscillating potentials with a zero mean is much more intriguing than that with a finite mean. In this section, we describe a practical setup that can be straightforwardly realized for ultracold atoms moving in optical lattices.

We start with two coherent laser beams, red-detuned from the atomic resonance, polarized in the same (e.g., vertical) direction, and intersecting at an acute angle  $2\alpha$ , as shown in Fig. 5. We assume that the beams are characterized by the angular frequency  $\omega$ , the wave number  $\kappa$ , and that the cross-sectional intensity profile is described by a Gaussian function of width  $b$ , i.e.,

$$I = I_0 \exp\left(-\frac{r_{\perp}^2}{2b^2}\right), \quad (30)$$

where  $r_{\perp}$  is distance of a given point from the central axis of the beam. Let us consider the setup where an external trapping

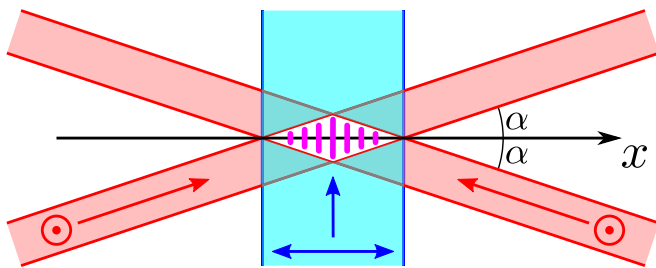


FIG. 5. Laser-beam configuration for the creation of an oscillating potential with zero mean. Two red-detuned beams, polarized in the direction perpendicular to their common plane of propagation, intersect at an angle  $2\alpha$  and create an interference pattern. An additional repulsive profile is created by a blue-detuned beam with in-plane polarization, propagating at the right angle to the  $x$  axis.

potential restricts the motion of ultracold atoms in the vicinity of the  $x$  axis. Near the  $x$  axis the respective electric fields created by the two beams are given by

$$E_1 = E_0 \cos(\omega t - \kappa x \cos \alpha) \exp\left[-\frac{x^2 \sin^2 \alpha}{2b^2}\right], \quad (31a)$$

$$E_2 = E_0 \cos(\omega t + \kappa x \cos \alpha) \exp\left[-\frac{x^2 \sin^2 \alpha}{2b^2}\right]. \quad (31b)$$

The resulting intensity distribution is given by the time-averaged square of the total electric field  $E_1 + E_2$ . Thus

$$\begin{aligned} I &\sim 2E_0^2 \cos^2(\kappa x \cos \alpha) \exp\left[-\frac{x^2 \sin^2 \alpha}{b^2}\right] \\ &= E_0^2 \{1 + \cos(2\kappa x \cos \alpha)\} \exp\left[-\frac{x^2 \sin^2 \alpha}{b^2}\right], \end{aligned} \quad (32)$$

and the resulting intensity distribution creates a rapidly oscillating potential profile with a slowly varying Gaussian envelope of a characteristic width  $b/\sin \alpha$  which may be much larger than the wavelength. Although this potential does not have a zero mean, the background contribution

$$V_{\text{bg}} \sim E_0^2 \exp\left[-\frac{x^2 \sin^2 \alpha}{b^2}\right] \quad (33)$$

can be canceled by applying an additional blue-detuned laser beam (see Fig. 5) polarized in the orthogonal direction and creating a broad Gaussian repulsive potential.

#### V. CONCLUSIONS AND OUTLOOK

We showed that quantum dynamics in potentials with fast spatial oscillations can be approximately described by a smoothed wave function that reproduces the overall structure of the true wave function but neglects its rapid small-scale oscillations. The equation of motion for the effective dynamics retains the form of the Schrödinger Eq. (20) and can be analyzed based on the usual framework and intuition available in single-particle quantum mechanics. In particular, generalizations to few- or many-particle problems can be readily made. In this context, it is intuitively clear that interparticle interactions will not be modified at large length scales; however, at short scales—comparable to the range of the performed averaging—interesting modifications may take place that are worth investigating in future work.

#### ACKNOWLEDGMENT

This research was supported by the Lithuanian Research Council under Grant No. APP-4/2016.

#### APPENDIX: ALTERNATIVE DERIVATION OF EFFECTIVE HAMILTONIAN

Here we derive the effective Schrödinger Eq. (20) for quantum dynamics in rapidly oscillating spatial potentials by using an alternative approach, inspired by an analogous treatment of classical motion in the presence of a rapidly oscillating force [25].

Our task is to approximately solve the Schrödinger equation

$$E\psi(x) = -\frac{d^2}{dx^2}\psi(x) + [kv(kx)\Phi(x) + \rho(x)]\psi(x), \quad (\text{A1})$$

with a slowly varying envelope function  $\Phi(x)$  and a rapidly oscillating function  $v(s)$  for a large but finite  $k$ . Anticipating the result obtained in the main text, we represent the wave function as a sum

$$\psi(x) = \bar{\psi}(x) + \xi(x) \quad (\text{A2})$$

of the smoothed wave function  $\bar{\psi}(x)$  and a correction  $\xi(x)$  that scales as  $k^{-1}$ . Substituting the wave function (A2) into the Schrödinger Eq. (A1) we obtain

$$E\bar{\psi} + E\xi = -\frac{d^2}{dx^2}\bar{\psi} - \frac{d^2}{dx^2}\xi + k\Phi v\bar{\psi} + k\Phi v\xi + \rho\bar{\psi} + \rho\xi, \quad (\text{A3})$$

which separates into two equations for oscillatory and smooth terms, respectively. Focusing first on the oscillating part

$$E\xi = -\frac{d^2}{dx^2}\xi + k\Phi v\bar{\psi} + k\Phi v\xi + \rho\xi, \quad (\text{A4})$$

we collect the terms that are of the order of  $k$  and arrive at a differential equation for the correction  $\xi(x)$ :

$$0 = -\frac{d^2}{dx^2}\xi + k\Phi v\bar{\psi}. \quad (\text{A5})$$

Assuming that  $\Phi$  and  $\bar{\psi}$  change slowly, the solution can be written as

$$\xi(x) = k^{-1}\Phi(x)\bar{\psi}(x)w(kx), \quad (\text{A6})$$

with  $w''(s) = v(s)$ ; here,  $w(s)$  is also a periodic function with zero mean. Averaging Eq. (A3) over one spatial period we obtain

$$E\bar{\psi} = -\frac{d^2}{dx^2}\bar{\psi} + k\Phi v\bar{\xi} + \rho\bar{\psi}. \quad (\text{A7})$$

Let us evaluate the average  $v\bar{\xi}$  in the second term on the right-hand side. Using Eq. (A6) we get

$$v\bar{\xi} = k^{-1}\Phi\bar{\psi}\langle vw \rangle = -k^{-1}\Phi\bar{\psi}\langle (w')^2 \rangle. \quad (\text{A8})$$

This leads to the result, equivalent to Eq. (20) since  $w'(s)$  is the antiderivative of  $v(s)$ , which is denoted  $g(s)$  in the main text.

- 
- [1] M. Born and R. Oppenheimer, *Ann. Phys. (Berlin, Ger.)* **389**, 457 (1927).
- [2] W. Kolsos, *Adv. Quantum Chem.* **5**, 99 (1970).
- [3] A. Eckardt, *Rev. Mod. Phys.* **89**, 011004 (2017).
- [4] C. Gross and I. Bloch, *Science* **357**, 995 (2017).
- [5] M. Aidelsburger, M. Atala, M. Lohse, J. T. Barreiro, B. Paredes, and I. Bloch, *Phys. Rev. Lett.* **111**, 185301 (2013).
- [6] H. Miyake, G. A. Siviloglou, C. J. Kennedy, W. C. Burton, and W. Ketterle, *Phys. Rev. Lett.* **111**, 185302 (2013).
- [7] M. Atala, M. Aidelsburger, M. Lohse, J. T. Barreiro, B. Paredes, and I. Bloch, *Nat. Phys.* **10**, 588 (2014).
- [8] M. Aidelsburger, M. Lohse, C. Schweizer, M. Atala, J. T. Barreiro, S. Nascimbène, N. R. Cooper, I. Bloch, and N. Goldman, *Nat. Phys.* **11**, 162 (2015).
- [9] C. J. Kennedy, W. C. Burton, W. C. Chung, and W. Ketterle, *Nat. Phys.* **11**, 859 (2015).
- [10] M. E. Tai, A. Lukin, M. Rispoli, R. Schittko, T. Menke, D. Borgnia, P. M. Preiss, F. Grusdt, A. M. Kaufman, and M. Greiner, *Nature (London)* **546**, 519 (2017).
- [11] N. Goldman and J. Dalibard, *Phys. Rev. X* **4**, 031027 (2014).
- [12] A. Eckardt and E. Anisimovas, *New J. Phys.* **17**, 093039 (2015).
- [13] V. Novičenko, E. Anisimovas, and G. Juzeliūnas, *Phys. Rev. A* **95**, 023615 (2017).
- [14] G. Jotzu, M. Messer, R. Desbuquois, M. Lebrat, T. Uehlinger, D. Greif, and T. Esslinger, *Nature (London)* **515**, 237 (2014).
- [15] A. G. Grushin, A. Gómez-León, and T. Neupert, *Phys. Rev. Lett.* **112**, 156801 (2014).
- [16] P. Windpassinger and K. Sengstock, *Rep. Prog. Phys.* **76**, 086401 (2013).
- [17] E. Witten, *Nucl. Phys. B* **188**, 513 (1981).
- [18] F. Cooper, A. Khare, and U. Sukhatme, *Phys. Rep.* **251**, 267 (1995).
- [19] F. Cooper, A. Khare, and U. Sukhatme, *Supersymmetry in Quantum Mechanics* (World Scientific, Singapore, 2001).
- [20] A. Gangopadhyaya, J. V. Mallow, and C. Rasinariu, *Supersymmetric quantum mechanics: An introduction* (World Scientific, Singapore, 2018).
- [21] D. E. Ruiz and I. Y. Dodin, *Phys. Rev. A* **95**, 032114 (2017).
- [22] V. Burd, *Method of Averaging for Differential Equations on an Infinite Interval* (Chapman and Hall/CRC, New York, 2007).
- [23] J. A. Sanders, F. Verhulst, and J. Murdock, *Averaging Methods in Nonlinear Dynamical Systems* (Springer, New York, 2007).
- [24] G. Pöschl and E. Teller, *Eur. Phys. J. A* **83**, 143 (1933).
- [25] L. D. Landau and E. M. Lifshitz, *Mechanics*, Course of Theoretical Physics, 3rd ed. (Butterworth-Heinemann, Oxford, 1976), Vol. 1.